



Open Access : : ISSN 1847-9286

<https://pub.iapchem.org/ojs/index.php/JESE>

Original scientific paper

Methanol oxidation at platinized copper particles prepared by galvanic replacement

Ioanna Mintsouli*, Jenia Georgieva**, Athanasios Papaderakis*, Stephan Armyanov**, Eugenia Valova**, Volodymyr Khomenko***, Stella Balomenou****, Dimitrios Tsiplakides*****, Sotiris Sotiropoulos*✉

*Department of Chemistry, Aristotle University of Thessaloniki, Thessaloniki 54124, Greece

**Rostislav Kaischew Institute of Physical Chemistry, Bulgarian Academy of Sciences, Sofia 1113, Bulgaria

***Kiev National University of Technologies and Design, Department for Electrochemical Power Engineering & Chemistry, Kiev 01011, Ukraine

****Chemical Process & Energy Resources Institute, Centre for Research and Technology Hellas, 570 01, Thessaloniki, Greece

✉Corresponding Author: eczss@chem.auth.gr; Tel.: +30-2310-997-742; Fax: +30-2310-997-709

Received: October 14, 2015; Accepted November 23, 2015

Abstract

Bimetallic Pt-Cu particles have been prepared by galvanic replacement of Cu precursor nanoparticles, upon the treatment of the latter with a chloro-platinate acidic solution. The resulting particles, typically a few tens of nm large, were supported on high surface area carbon (Vulcan® XC-72R, Cabot) and tested as electrodes. Surface electrochemistry in deaerated acid solutions was similar to that of pure Pt, indicating the existence of a Pt shell (hence the particles are denoted as Pt(Cu)). Pt(Cu)/C supported catalysts exhibit superior carbon monoxide and methanol oxidation activity with respect to their Pt/C analogues when compared on a per electroactive surface area basis, due to the modification of Pt activity by Cu residing in the particle core. However, as a result of large particle size and agglomeration phenomena, Pt(Cu)/C are still inferior to Pt/C when compared on a mass specific activity basis.

Keywords

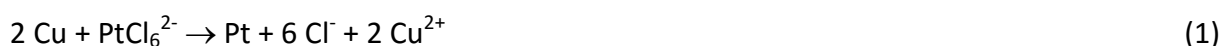
Transmetalation; Electrocatalysts; Platinum

Introduction

The need for reducing the cost and at the same time maintaining or improving the performance of catalysts used in fuel cells and electrolyzers has led to intensive research into non-precious me-

tal alternatives or multi-metallic noble-metal-based systems. All common preparation methods for the latter involve a reduction step, either using a reducing agent in solution phase or in a reducing atmosphere (e.g. hydrogen) at elevated temperatures [1-5]. A high surface area support (usually carbon) is either present in the catalyst synthesis mixture or added during a subsequent step.

Since the appearance of the first papers on the subject [6-12], galvanic replacement has been established during the last decade as an alternative method for preparing multi-metallic noble-metal-based electrode materials. The principle of the method lies on the fact that when a non-noble metal (e.g. Pb, Cu, Fe, Co, Ni, Mo, Bi) is immersed in a solution containing ions of a noble metal (e.g. Pt, Au, Pd, Ir, Ru) then, due to a difference in standard potentials, the latter is deposited in metallic form replacing layers of the former (which is oxidized/released in ionic form in the solution). An example of the process for Cu and Pt, resulting in a Pt-rich shell and a Cu-containing core (denoted as Pt(Cu)), is given by reaction (1) below:



Among advantages of the technique one can mention its room temperature conditions, the use of dilute solutions of the precious metal, as well as the potential formation of a noble-metal-rich shell / bimetallic-core structure. The latter can reduce the amount of the precious metal in the catalyst and also lead to beneficial electronic effects of the second metal on its catalytic activity. There have been three main research groups in the area. Adzic and co-workers have put emphasis on the replacement of Cu UPD monolayers by precious metals and the catalysis of oxygen reduction (see for example [8-10,13-19]); Kokkinidis, Sotiropoulos and co-workers have used the replacement of surface layers of transition metal deposits by Pt, mostly for methanol oxidation catalysis and with a recent emphasis on catalyst preparation on carbon and semiconductor oxide high surface area supports [11-12,20-33]; finally, Podlovchenko and co-workers have focused on the replacement of Cu or Mo layers by Pt or Pd and their use as methanol and formic acid oxidation catalysts [34-39].

Methanol oxidation in acid is the fuel reaction in direct methanol fuel cells (see for example [40-41]) which are envisaged as candidates for portable/micro-fuel cells. To improve tolerance towards CO intermediate poisoning, multi-metallic systems based on Pt have long been explored. Foreign metals adsorbed as ad-atoms or alloyed with Pt have been extensively studied (see for example [42-46]). We have tested the catalytic activity of Pt(Pb) [20] and Pt(Cu), Pt(Ni), Pt(Co) [26] core-shell catalytic layers on glassy carbon electrodes and have found a pronounced activity and stability of the Pt(Cu) formulations towards methanol oxidation. A rather limited number of papers of Pt(Cu) particles prepared by chemical methods on C particle supports can be found in the literature [29-33,47-52], which include those by our group [29-33]. In all but a few of these works [48,49,52] galvanic replacement occurred after the Cu precursor was cast on the C support or in the presence of the latter. As discussed in [29], the presence of the conducting C particles provides an alternative location for Pt deposition (to that of the surface of Cu): electrons released from Cu dissolving in the solution can travel through C to nearby locations whereby Pt ions can be reduced and deposited as metallic Pt. In that case the catalyst comprises of a mixture of Pt(Cu) and pure Pt particles, moderating the beneficial effect of Cu on Pt catalytic activity. However, if the Pt(Cu) particles were first to be synthesized and then mixed with/anchored on the C particles one would ensure the bimetallic character of the catalyst.

The aim of this work has been to prepare Pt(Cu) bimetallic particles by the galvanic replacement technique and then use them as supported catalysts for methanol oxidation. Specific

objectives have been: *i.* The preparation of Cu nanoparticles and their conversion into platinized bimetallic particles; *ii.* The microscopic, spectroscopic and crystallographic characterization of the Pt(Cu) and Pt(Cu)/C materials; *iii.* The electrochemical characterization of the deposits by means of Pt surface electrochemistry in acid, CO oxidation and methanol oxidation.

Experimental

a. Preparation of Cu and Pt(Cu) nanoparticles and Pt(Cu)/C modified electrodes

The Cu powder was prepared by reduction in a hydrogen-containing recirculate gas stream. The required amount of $\text{Cu}(\text{NO}_3)_2 \cdot 3\text{H}_2\text{O}$ was dissolved in a 1:1 water-ethanol mixture and heated at 80°C for 1 h 30 min under stirring until complete solvent evaporation. The resulting solid was crushed in a mortar and then placed in a crucible and thermally treated for 60 min at 300°C in an Ar atmosphere for CuO formation. In our experiments metallic copper powder was obtained by the reaction of CuO at 250°C under a 8 % H_2 /92 % Ar mixture (gas flow $20\text{ cm}^3/\text{min}$) for 60 min. Finally, the powder was left to cool to room temperature under Ar.

In a typical process, 0.05 g of freshly prepared Cu particles were added in 25 ml of a $5 \times 10^{-3}\text{ M}$ $\text{K}_2\text{PtCl}_6 + 0.1\text{ M HCl}$ deaerated solution and were sonicated for 45 min in an ultrasound bath so that spontaneous partial replacement of Cu by Pt could take place:



((Cu) denotes copper in the bulk/core of the particles).

Finally, the suspension is filtered to obtain ca 0.022 g of a black powder product (Pt(Cu)). Note that the filtrate has turned light blue (indicative of the release of Cu ions according to (2)) from the originally light yellow colour of the suspension (due to K_2PtCl_6). 0.0173 g of the Pt(Cu) powder were mixed with 0.0692 g of carbon powder (Vulcan® XC-72R Cabot) so that the mixture was 20 % w/w in the catalyst. The Pt(Cu)/C mixture was dispersed in 1 ml ethanol and was ultrasonicated for 5 min and then left to dry.

For the electrochemical testing of the catalyst, 3 mg of the thus prepared Pt(Cu)/C material (or of commercial 20% w/w Pt/C catalyst, ETEK) were suspended in 0.5 ml methanol together with drops of a Nafion® (protonic form) 5 % w/w solution in a mixture of low aliphatic alcohols and 45% water (Aldrich), amounting to 2.5 mg of Nafion® polymer. The as prepared suspension was homogenized in an ultrasonic bath and a given quantity of the slurry (containing the desired catalyst + support weight in the 0.8-1 mg range) was placed in a drop-wise manner on a flat glassy carbon electrode (GC, BAS Inc.) over a total area of 0.385 cm^2 and left to dry. The resulting Pt loading in the Pt(Cu)/C electrode whose results are presented here (based on the EDS analysis of the catalyst, see also below) was $0.20\text{ mg}_{\text{Pt}}\text{ cm}^{-2}$; that of the 20 % w/w Pt/C commercial catalyst was $0.43\text{ mg}_{\text{Pt}}\text{ cm}^{-2}$.

b. Microscopic, spectroscopic and crystallographic characterisation of materials

Scanning Electron Microscopy (SEM) was carried out using a JEOL JSM-5510 microscope and elemental analysis of the coatings was performed by the accompanying EDS (EDAX) system. The morphology of the catalysts was investigated with high resolution transmission electron microscopy (TEM) using a JEOL JEM 2010 microscope coupled with Oxford INCA X-ray EDS. X-Ray Diffraction (XRD) deposit characterisation was performed with the help of a Rigaku Miniflex diffractometer.

c. Electrochemical experiments

Voltammetry was carried out with an Autolab 30 (EcoChimie) system in a three-electrode cell. A saturated calomel electrode (SCE) was used as the reference electrode and a Pt foil as the counter electrode.

The catalytic electrode was first scanned in a deaerated 0.1 M HClO₄ solution between the hydrogen and oxygen evolution potential limits at 500 mV s⁻¹ until a steady state voltammetric picture was recorded (typically after 20-30 cycles, whereby anodic currents due to uncovered Cu dissolution vanished). Next, the electrode was scanned again in a fresh deaerated 0.1 M HClO₄ solution at 10 mV s⁻¹, for a steady state voltammogram (typical of Pt) to be attained (typically after 2–3 cycles). Following that, the solution was saturated with pure CO gas (>99.99 % purity; Air Liquide) and the electrode was polarized at +0.10 V vs. SCE for 5 min (for CO adsorption to take place) and then scanned to more positive potentials at 50 mV s⁻¹ (for CO oxidative removal). Finally, the electrode was scanned in a 0.5 MeOH + 0.1 M HClO₄ solution at 5 mV s⁻¹ to study the methanol oxidation reaction.

d. Chemicals

Cu(NO₃)₂·3H₂O from Sigma-Aldrich (ACS reagent) was used in the precursor solutions for Cu particle preparation. H₂PtCl₆ hexahydrate from Sigma-Aldrich (ACS reagent, ≥37.50 % as Pt) was employed for the Pt exchange solution. MeOH was from Riedel (Chromasolv[®], for HPLC, gradient grade, ≥99.9 %). HClO₄ from Riedel, (*puriss p.a.*, ACS reagent, ≥70 %) was added both in the galvanic replacement solution and as the supporting electrolyte in MeOH oxidation experiments.

Results and discussion

a. Microscopic, spectroscopic and crystallographic characterisation of Cu, Pt(Cu) and Pt(Cu)/C particles

Figure 1 shows the XRD diffractogram of the freshly prepared Cu nanoparticles. It can be seen that these are made of metallic Cu, as expected for a material annealed in a reductive atmosphere (see Experimental). The average crystallite size could be estimated as 43 nm, using Scherrer's formula for the sharp $2\theta_{\text{Cu}(111)} = 43.4501$ degrees peak. It should be noted that, despite prolonged ultrasonic treatment of Cu particle suspensions in ethanol, these were heavily aggregated and no individual particles or even nano-sized aggregates could be identified by TEM microscopy.

Figure 2 is a SEM micrograph of the filter cake of as prepared Pt(Cu) material, prepared by the partial galvanic replacement of Cu by Pt. The as prepared material is particulate and consists of aggregates smaller than 1 μm. EDS analysis gave a Pt÷Cu÷O atomic ratio of 22÷70÷8, indicating a Cu-rich material (with some Cu oxides also formed during galvanic replacement or/and prolonged exposure to atmosphere).

Figure 3 presents the XRD diffractogram of the Pt(Cu) catalyst and the wide peaks correspond to small crystallites, estimated to have an average size of ca 4 nm, using Scherrer's formula. The shrinkage of crystallites from 43 to 4 nm as one passes from Cu to Pt(Cu) is in line with Cu dissolving as Pt deposits on its surface according to the galvanic replacement mechanism. The shift of the Pt peaks to lower θ values is indicative of alloy formation between Pt and a metal with a smaller lattice constant such as Cu. Using Vegard's law, the atomic composition of the alloy is estimated as Pt÷Cu = 73÷27. Comparing this composition with that of the EDS results (22÷70) it follows that a large part of Cu remains non-alloyed, most likely as very small pockets of amorphous material within the Pt(Cu) particles; the degree of alloying can thus estimated not to exceed 37% and expected to be restricted to the outer part of the particles.

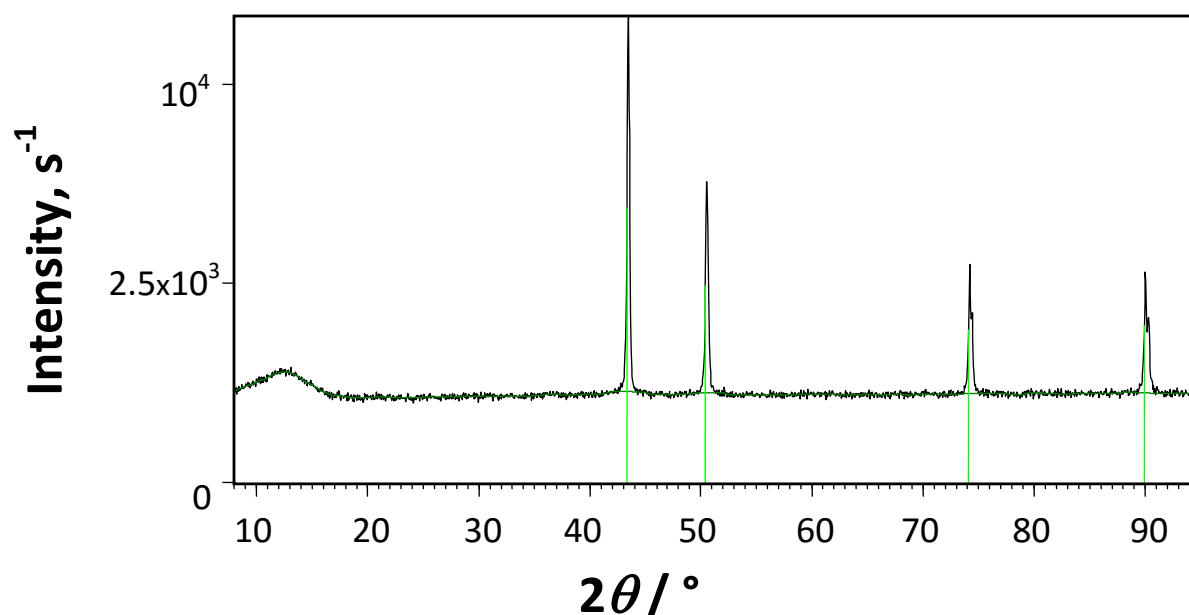


Figure 1. XRD diffractogram (of Cu particles prepared by hydrothermal treatment of $\text{Cu}(\text{CH}_3\text{COO})_2$ followed by high temperature reduction in a hydrogen atmosphere (see Experimental)

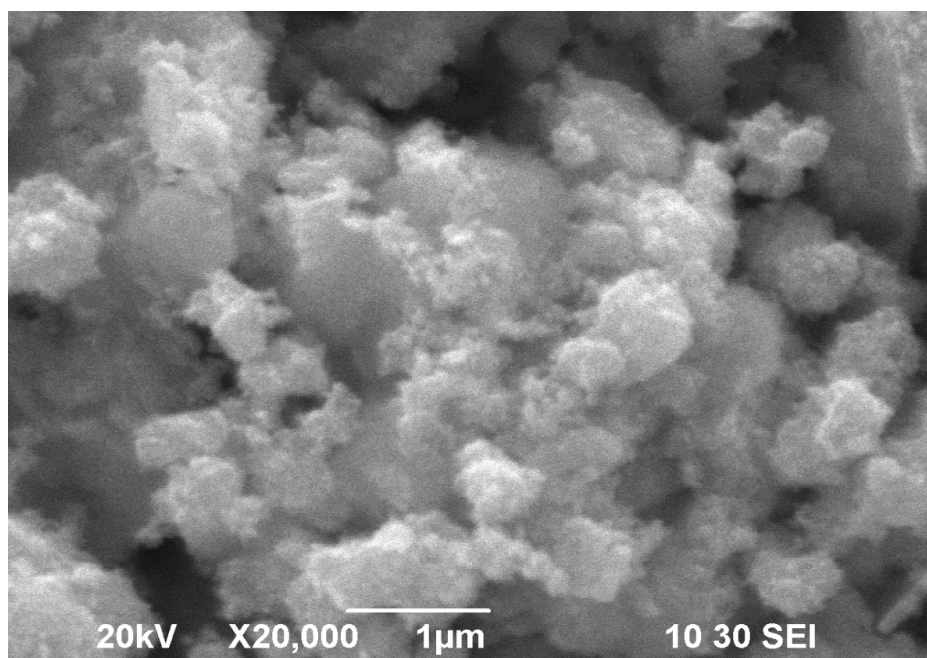


Figure 2. SEM micrographs of the filter cake of Pt(Cu) particles, prepared by hydrothermal treatment of $\text{Cu}(\text{CH}_3\text{COO})_2$ followed by high temperature reduction in a hydrogen atmosphere (see Experimental)

Figure 4 shows TEM micrographs of a Pt(Cu) large aggregate (A) and of detached smaller aggregates of the material (B), following dispersion of the Pt(Cu) filtrate of Figure 2 in ethanol (with magnetic stirring). The smaller particles are spherical in shape with dimensions in the 20-30 nm range and they seem to consist of even smaller particles; the atomic composition of each individual particle is found by EDS to be Pt÷Cu=30÷70, in line with what was found for the material as a whole (see above).

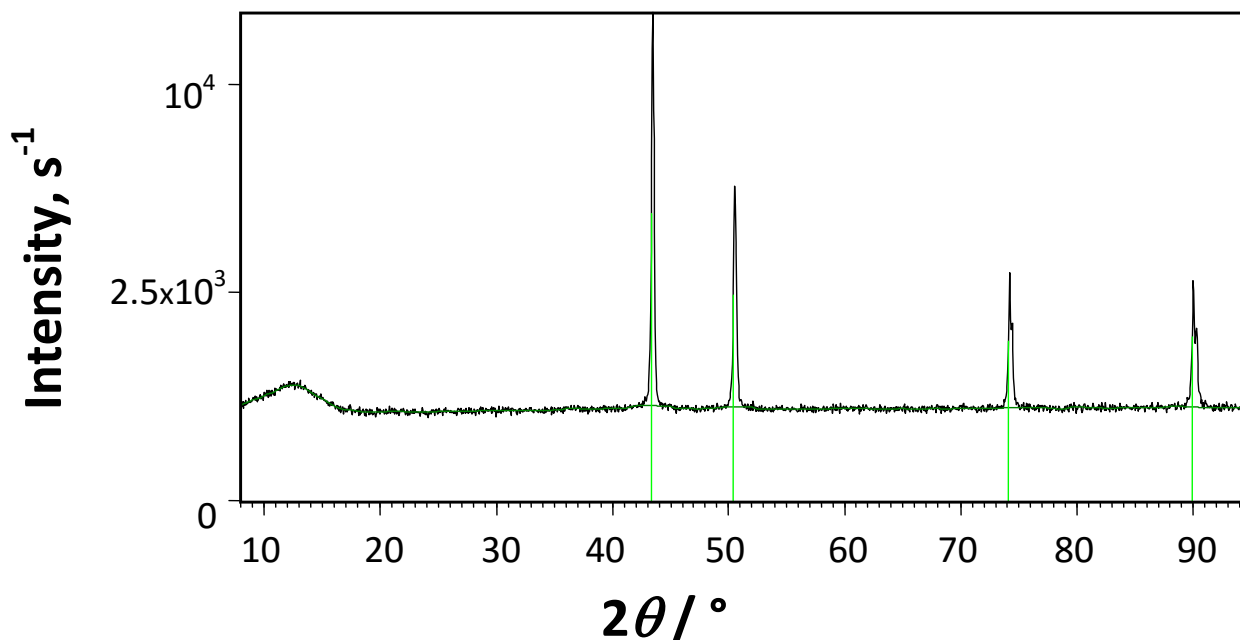


Figure 3. XRD diffractogram of Pt(Cu) particles prepared by galvanic replacement of Cu particles' surface upon immersion of the latter in a solution containing Pt in ionic form (see Experimental)

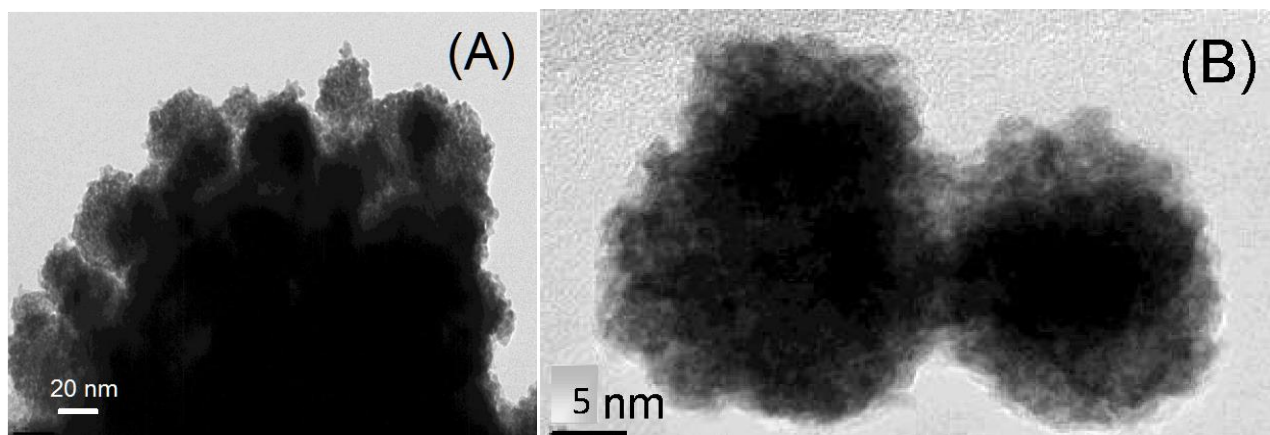


Figure 4. TEM micrographs of Pt(Cu) particles prepared by galvanic replacement of Cu particles' surface upon immersion of the latter in a solution containing Pt in ionic form (see Experimental); (A) Micrograph of a large aggregate, (B) Micrograph of individual particles

Figure 5 shows TEM micrographs of the Pt(Cu) particles supported on /mixed with C particles by means of ultrasonic treatment in ethanol. In Figure 5(A) the spherical carbon support particles are seen, having a fairly even size distribution of ca. 30 nm. Figure 5(B) reveals the scatter of small (less than 20 nm in diameter) Pt(Cu) particles (seen as dark spots) in the Pt(Cu)/C system, whereas Figure 5(C) depicts in more detail an individual such particle. The observed morphology of individual particles is in line with the expected deposition of Pt clusters on top of a Cu rich core. Figure 5(D) shows the Pt nanoparticles of a commercial Pt/C catalyst made of very small nanoparticles (2-3 nm) with limited aggregation phenomena.

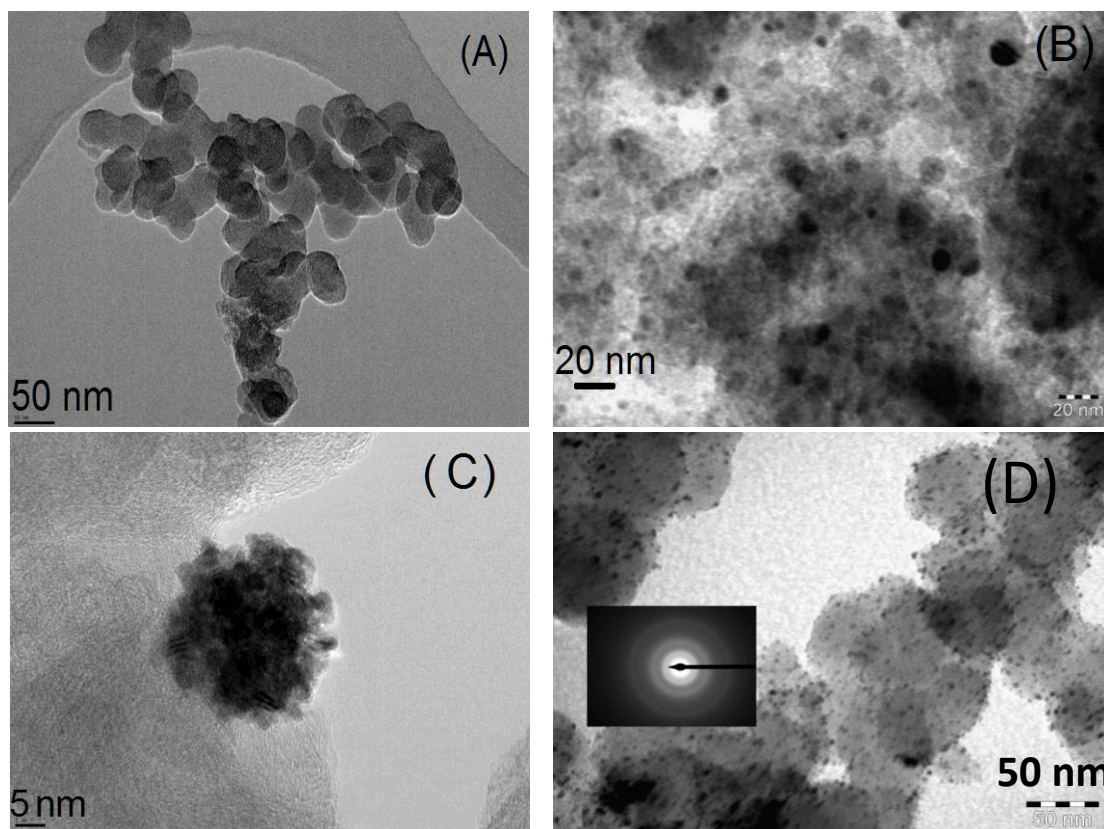


Figure 5. TEM micrographs of Pt(Cu) particles supported on carbon particles (Pt(Cu)/C) (see Experimental); (A), (B), (C) Micrographs at different magnifications as indicated by the scale bars. For comparison, a micrograph for commercial 20% w/w Pt/C catalyst (Etek) is shown in (D)

b. Electrochemical characterisation of Pt(Cu)/C in acid

Figure 6 presents the stabilized picture (see Experimental) of cyclic voltammograms of the Pt(Cu)/C and Pt/C electrodes, obtained at 50 mVs^{-1} in acid. Both electrodes show the typical hydrogen adsorption/desorption and oxide formation/stripping features of high surface area-carbon-supported Pt. This is macroscopic evidence that the outer surface of the Pt(Cu) catalyst is made of a pure, protective Pt shell.

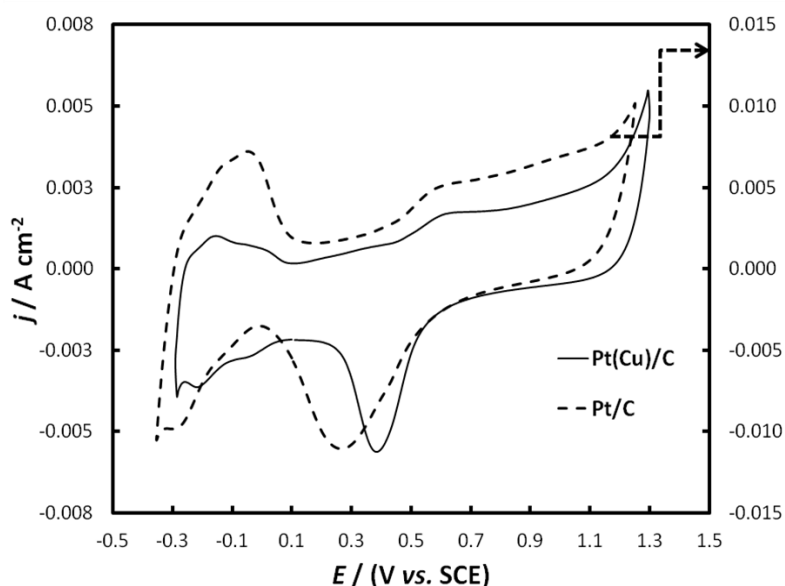


Figure 6. Cyclic voltammograms (50 mV s^{-1} potential scan rate) of Pt(Cu)/C and Pt/C electrodes in deaerated 0.1 M HClO_4

Two further points can be made: first, the hydrogen peak area (between +0.1 and -0.3 V) is smaller for the Pt(Cu) electrode, as expected for a low specific area due to larger particles and aggregation phenomena (Figure 5); second, the ill-defined hydrogen peak area (typical of carbon-supported Pt nanoparticles) does not allow for a reliable estimate of the catalyst electroactive area (from the charge corresponding to the area under the cathodic or anodic part of the curve in that range, associated with adsorption and desorption of a H monolayer).

In order to obtain a more accurate estimate of the catalyst electroactive area we therefore resort to the oxidative removal of a pre-adsorbed CO monolayer during the positive-going potential scan of the voltammograms shown in Figure 7 (see also Experimental). The anodic charge between ca +0.4 and +0.7 V corresponds to the oxidation of a full CO monolayer and is associated with a charge density of $420 \mu\text{C cm}^{-2}$ of Pt [53]. The Pt electroactive area (per electrode substrate geometric area) of the catalyst layers can thus be calculated as $5.19 \text{ cm}^2 \text{ cm}^{-2}$ for Pt(Cu)/C and $77.92 \text{ cm}^2 \text{ cm}^{-2}$ for Pt/C. The mass specific electroactive areas in the prepared coatings can then be estimated (based on the Pt loadings-see Experimental) as 2.6 and $18.1 \text{ m}^2 \text{ g}^{-1}$ respectively. (Such low values can be interpreted by extensive agglomeration taking place in coatings with relatively large catalyst loadings; note that ca 1mg of catalyst and support were loaded over a 0.385 cm^2 surface, resulting in a ca 2.5 mg cm^{-2} of catalyst+support total loading).

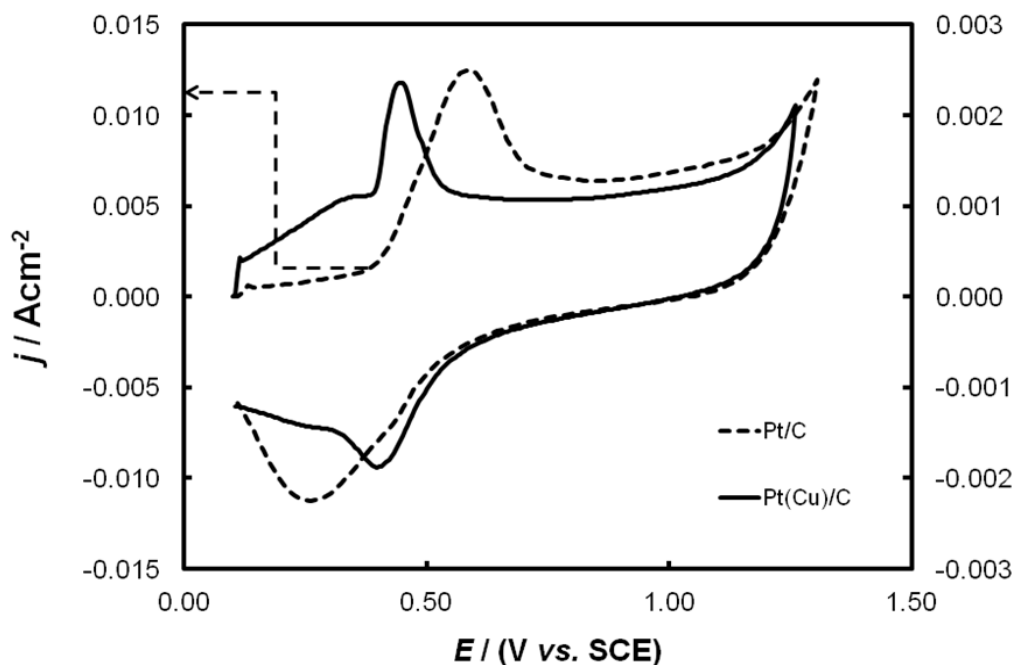


Figure 7. Cyclic voltammograms (50 mV s^{-1} potential scan rate) of Pt(Cu)/C and Pt/C electrodes in a deaerated 0.1 M HClO_4 , following CO pre-adsorption from a CO-saturated solution

The most interesting feature of the voltammograms of Figure 7 is the ca 150 mV negative shift of the CO oxidation peak in the case of the Pt(Cu) catalyst, proving its better catalytic activity for CO oxidation. Note that this is higher than the shift obtained at other Pt(Cu) systems prepared by galvanic replacement where C was present during the replacement step (and thus some of Pt was deposited directly on C and remained without strong Pt-Cu interactions) [29,30].

Figure 8 presents the positive-going voltammogram corresponding to methanol oxidation, with the current density, j_e , reported per Pt electroactive surface area as obtained from the results of Figure 7. It can be seen that the intrinsic activity (corrected for mere surface area effects) of the Pt(Cu) catalyst is superior to that of plain Pt catalysts, highlighting the beneficial effect of Pt-Cu

interactions on methanol oxidation, presumably because of its ability to remove the CO poisonous intermediate, in line with the findings of the oxidative CO removal discussed above. The current density obtained is the highest among similar catalysts [29,30].

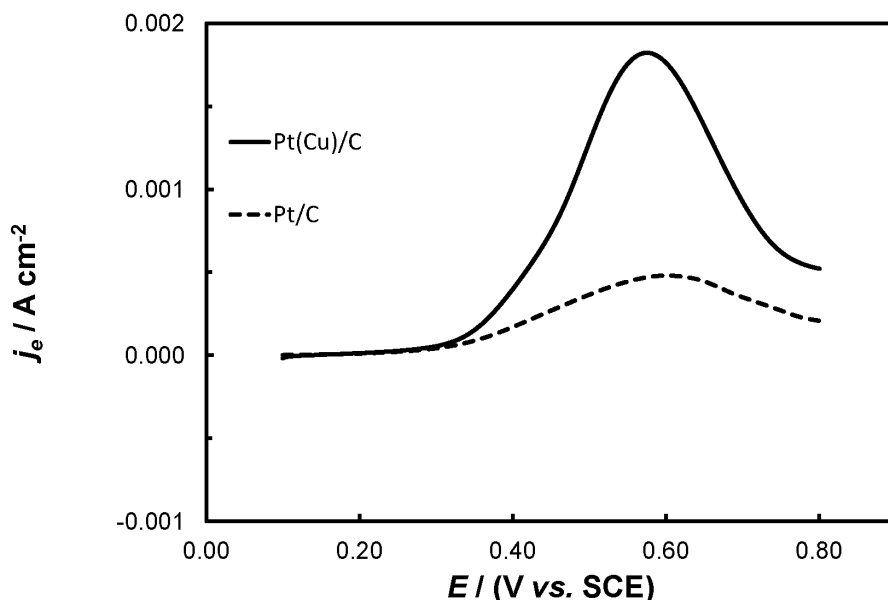


Figure 8. Voltammograms (5 mV s^{-1} potential scan rate; positive going scan) of Pt(Cu)/C and Pt/C electrodes in $0.5 \text{ M MeOH} + 0.1 \text{ M HClO}_4$ solutions; current densities, j_e , are per electroactive surface area

In Figure 9 the positive-going voltammograms for methanol oxidation are shown again, where the current density, j_m , is now reported per mass of Pt. In this case, the commercial catalyst appears to be better since the effect of very low surface area of Pt(Cu) (see large particles and agglomerates in Figure 5) overrides its higher intrinsic catalytic activity.

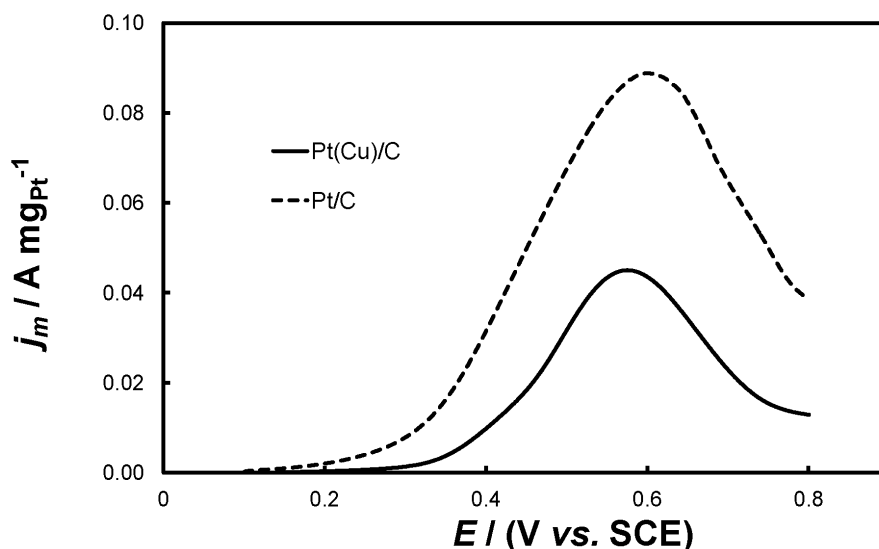


Figure 9. Voltammograms (5 mV s^{-1} potential scan rate; positive going scan) of Pt(Cu)/C and Pt/C electrodes in $0.5 \text{ M MeOH} + 0.1 \text{ M HClO}_4$ solutions; current densities, j_m , are per mass of Pt

Conclusions

- i. Bimetallic Pt-Cu catalysts have been prepared by partial galvanic replacement of Cu nanoparticles synthesized by a precipitation/reduction method. The catalyst was then supported on a high surface area C powder.

- ii. Following electrochemical treatment in acid the voltammetric picture of the Pt(Cu)/C electrode was similar to that of a pure Pt/C one, indicating the formation of a protective outer Pt shell over a Cu-containing core (Pt(Cu)).
- iii. The Pt(Cu)/C electrodes have superior intrinsic catalytic activity towards CO oxidation and methanol oxidation in acid.
- iv. Due to the formation of large Pt(Cu) particles and extensive agglomeration, the bimetallic catalyst exhibited a low electroactive surface area and hence a moderate mass specific activity.
- v. Future research should be directed towards the preparation of smaller Pt(Cu) bimetallic nanoparticles (possibly by the synthesis of smaller Cu particle precursors) so that not only the intrinsic catalytic activity is improved (due to Pt-Cu interactions) but also the overall, mass specific activity increases significantly (due to a higher surface area).

Acknowledgements: This research has been co-financed by the European Union (European Social Fund – ESF) and Greek national funds through the Operational Program "Education and Lifelong Learning" of the National Strategic Reference Framework (NSRF) - Research Funding Program: Heracleitus II. Investing in knowledge society through the European Social Fund.

References

- [1] E. Antolini, *Appl. Catal. B: Env.* **74** (2007) 324
- [2] E. Antolini, *J. Mater. Sci.* **38** (14) (2003) 2995
- [3] C. R. K. Rao, D. C. Trivedi, *Coordination Chem. Rev.* **249** (2005) 613
- [4] H. Bonnemann, W. Brixoux, R. Brinkmann, E. Dinjus, T. Jouben, B. Korall, *Angew. Chem. Int. Ed. Engl.* **30** (1991) 1312
- [5] M. Boutonnet, J. Kizling, P. Stenius, G. Maire, *Colloids Surf.* **5** (1982) 209
- [6] G. Kokkinidis, A. Papoutsis, D. Stoychev, A. Milchev, *J. Electroanal. Chem.* **486** (2000) 48
- [7] G. Kokkinidis, D. Stoychev, V. Lazarov, A. Papoutsis, A. Milchev, *J. Electroanal. Chem.* **511** (2001) 20
- [8] S. R. Brankovic, J. X. Wang, R. R. Adzic, *Surf. Sci.* **474** (2001) L173
- [9] S. R. Brankovic, J. McBreen, R. R. Adzic, *J. Electroanal. Chem.* **503** (2001) 99
- [10] S. R. Brankovic, J. McBreen, R.R. Adzic, *Surf. Sci.* **479** (2001) L363
- [11] M. Van Brussel, G. Kokkinidis, I. Vandendael, C. Buess-Herman, *Electrochem. Commun.* **4** (10) (2002) 808
- [12] M. Van Brussel, G. Kokkinidis, A. Hubin, Cl. Buess-Herman, *Electrochim. Acta* **48** (2003) 3909
- [13] K. Sasaki, Y. Mo, J. X. Wang, M. Balasubramanian, F. Uribe, J. McBreen, R. R. Adzic, *Electrochim. Acta* **48** (25-26) (2003) 3841
- [14] K. Sasaki, J. X. Wang, M. Balasubramanian, J. McBreen, F. Uribe, R. R. Adzic, *Electrochim. Acta* **49** (22-23) (2004) 3873
- [15] J. Zhang, M. B. Vukmirovic, K. Sasaki, A. U. Nilekar, M. Mavrikakis, R. R. Adzic, *J. Am. Chem. Soc.* **127** (36) (2005) 12480
- [16] J. Zhang, F. H. Lima, M. H. Shao, K. Sasaki, J. X. Wang, J. Hanson, R. R. Adzic, *J. Phys. Chem. B* **109**(48) (2005) 22701
- [17] R. R. Adzic, J. Zhang, K. Sasaki, M. B. Vukmirovic, M. Shao, J. X. Wang, A. U. Nilekar, M. Mavrikakis, J. A. Valerio, F. Uribe, *Top. Catal.* **46** (2007) 249
- [18] Y. Ando, K. Sakaki, R. Adzic, *Electrochem. Commun.* **11** (2009) 1135
- [19] K. Sasaki, H. Naohara, Y. Cai, Y. M. Choi, P. Liu, M. B. Vukmirovic, J. X. Wang, R.R. Adzic, *Ang. Chem. Int. Ed.* **49** (46) (2010) 8602

- [20] S. Papadimitriou, A. Tegou, E. Pavlidou, G. Kokkinidis, S. Sotiropoulos, *Electrochim. Acta* **52** (2007) 6254
- [21] A. Tegou, S. Papadimitriou, E. Pavlidou, G. Kokkinidis, S. Sotiropoulos, *J. Electroanal. Chem.* **608** (2007) 67
- [22] S. Papadimitriou, A. Tegou, E. Pavlidou, G. Kokkinidis, S. Sotiropoulos, *Electrochim. Acta* **53** (2008) 6559
- [23] A. Tegou, S. Papadimitriou, S. Armyanov, E. Valova, G. Kokkinidis, S. Sotiropoulos, *J. Electroanal. Chem.* **623** (2) (2008) 187
- [24] A. Tegou, S. Armyanov, E. Valova, O. Steenhaut, A. Hubin, G. Kokkinidis, S. Sotiropoulos, *J. Electroanal. Chem.* **634** (2) (2009) 104
- [25] A. Tegou, S. Papadimitriou, G. Kokkinidis, S. Sotiropoulos, *J. Solid State Electrochem.* **14** (2) (2010) 175
- [26] S. Papadimitriou, S. Armyanov, E. Valova, A. Hubin, O. Steenhaut, E. Pavlidou, G. Kokkinidis, S. Sotiropoulos, *J. Phys. Chem. C* **114** (11) (2010) 5217
- [27] A. Tegou, S. Papadimitriou, I. Mintsouli, S. Armyanov, E. Valova, G. Kokkinidis, S. Sotiropoulos, *Catalysis Today* **170** (1) (2011) 126
- [28] I. Mintsouli, J. Georgieva, E. Valova, S. Armyanov, A. Kakaroglou, A. Hubin, O. Steenhaut, J. Dille, A. Papaderakis, G. Kokkinidis, S. Sotiropoulos, *J. Solid State Electrochem.* **17** (2) (2013) 435
- [29] I. Mintsouli, J. Georgieva, S. Armyanov, E. Valova, G. Avdeev, A. Hubin, O. Steenhaut, J. Dille, D. Tsiplakides, S. Balomenou, S. Sotiropoulos, *Appl. Catal. B: Env.* **136-137** (2013) 160
- [30] J. Georgieva, E. Valova, I. Mintsouli, S. Sotiropoulos, S. Armyanov, A. Kakaroglou, A. Hubin, O. Steenhaut, J. Dille, *J. Appl. Electrochem.* **44** (2) (2014) 215
- [31] B. Geboes, I. Mintsouli, B. Wouters, J. Georgieva, A. Kakaroglou, S. Sotiropoulos, E. Valova, S. Armyanov, A. Hubin, T. Breugelmans, *Appl. Catal. B: Env.* **150-151** (2014) 249
- [32] J. Georgieva, S. Sotiropoulos, E. Valova, S. Armyanov, N. Karanasios, *J. Electroanal. Chem.* **727** (2014) 135
- [33] J. Georgieva, E. Valova, I. Mintsouli, S. Sotiropoulos, D. Tatchev, S. Armyanov, A. Hubin, J. Dille, A. Hoell, V. Raghuwanshi, N. Karanasios, L. Malet, *J. Electroanal. Chem.* **754** (2015) 65
- [34] B. I. Podlovchenko, T. D. Gladysheva, A. Y. Filatov, L. V. Yashina, *Russ. J. Electrochem.* **46** (10) (2010) 1189
- [35] V. V. Kuznetsov, B. I. Podlovchenko, K. V. Kavyrshina, Yu M. Maksimov, *Russ. J. Electrochem.* **46** (12) (2010) 1353
- [36] B. I. Podlovchenko, U. E. Zhumaev, Y. M. Maksimov, *J. Electroanal. Chem.* **651** (1) (2011) 30
- [37] B. I. Podlovchenko, V. A. Krivchenko, Yu M. Maksimov, T. D. Gladysheva, L. V. Yashina, S. A. Evlashin, A. A. Pilevsky, *Electrochim. Acta* **76** (2012) 137
- [38] B. I. Podlovchenko, Y. M. Maksimov, K. I. Maslakov, *Electrochim. Acta* **130** (2014) 351
- [39] B. I. Podlovchenko, Y. M. Maksimov, S. A. Evlashin, T. D. Gladysheva, K. I. Maslakov, V. A. Krivchenko, *J. Electroanal. Chem.* **743** (2015) 93
- [40] C. Lamy, J. -M. Léger, S. Srinivasan, in J. O. M. Bockris, B. E. Conway (Eds.), *Modern Aspects of Electrochemistry*, **Vol.34**, Plenum Press, NY, 2000, Ch.3, p. 53
- [41] A. Hamnett, in W. Vielstich, A. Lamm, H. A. Gasteiger (Eds.), *Handbook of Fuel Cells: Fundamentals Technology and Applications*, Wiley, Chichester, 2003, **Vol.1**, Ch.18, p. 305
- [42] B. Beden, F. Kadirgan, C. Lamy, J. -M. Léger, *J. Electroanal. Chem.* **127** (1981) 75
- [43] H. Zhao, L. Li, J. Yang, Y. Zhang, *Electrochem. Commun.* **10** (2008) 1527
- [44] M. K. Jeon, J. S. Cooper, P. J. McGinn, *J. Power Sources* **185** (2008) 913
- [45] Y. J. Kuang, B. H. Wu, Y. Cui, Y. M. Yu, X. H. Zhang, J. H. Chen, *Electrochim. Acta* **56** (2011) 8645
- [46] X. Yu, D. Wang, Q. Peng, Y. Li, *Chem. Commun.* **47** (2011) 8094

- [47] A. Sarkar, A. Manthiram, *J. Phys. Chem. C* **114** (2010) 4725
- [48] C. Du, M. Chen, W. Wang, Q. Tan, K. Xiong, C. Yin, *J. Power Sources* **240** (2013) 630
- [49] Q. Li, P. Xu, B. Zhang, G. Wu, H. Zhao, E. Fu, H. Wang, *Nanoscale* **5** (16) (2013) 7397
- [50] J. M. Sieben, A. E. Alvarez, V. Comignani, M. M. E. Duarte, *Int. J. Hydrogen Energy* **39** (22) (2014) 11547
- [51] J. M. Sieben, A. E. Alvarez, V. Comignani, M. M. E. Duarte, *Int. J. Hydrogen Energy* **39** (16) (2014) 8667
- [52] Y. -X. Wang, H. -J. Zhou, P. -C. Sun, T. -H. Chen, *J. Power Sources* **245** (2014) 663
- [53] R. W. Lindström, K. Kortsdottir, M. Wesselmark, A. Oyarce, C. Lagergren, G. Lindbergh, *J. Electrochem. Soc.* **157** (12) (2010) B1795

© 2016 by the authors; licensee IAPC, Zagreb, Croatia. This article is an open-access article distributed under the terms and conditions of the Creative Commons Attribution license

<http://creativecommons.org/licenses/by/4.0/>

